Metal-Coated Zinc Oxide Nanocavities

Chi-Yu Adrian Ni, Shu-Wei Chang, *Member, IEEE*, Daniel J. Gargas, Michael C. Moore, Peidong Yang, and Shun Lien Chuang, *Fellow, IEEE*

***Abstract*— We theoretically demonstrate that metals can be useful for increasing the quality factor and confinement factor of a zinc oxide (ZnO) nanocavity. For small cavities, the advantages of low radiation loss and significant mode confinement due to metal coating outweigh the disadvantage of absorption loss from metal and efficiently lower the threshold material gain. The performances of ZnO cavities without metal coating, with aluminum (Al) coating, and with silver (Ag) coating are investigated. The results indicate that while surface-wave-like *plasmonic modes* are lossy due to metal loss, the performances of well-confined *dielectric modes* are indeed improved significantly as a result of metal. Both Al and Ag can significantly reduce the threshold material gain of the uncoated ZnO cavity from 16 613 cm^{-1} to less than 5000 cm^{-1}. In particular, the threshold material gain of Ag-coated cavity is reduced to only 3206 cm^{-1}.**

***Index Terms*— Finite difference time domain, nanocavities, plasmonics, zinc oxide.**

I. Introduction

NANOLASERS are desirable due to their small power consumption and the potential for advanced applications such as fast-switching optical logic circuits and biosensing. However, the challenge lies in the design of a nanocavity with both a high-quality (Q) factor and large energy confinement factor Γ_E [1]. When the dimension of the cavity is close to the resonant wavelength, the field tends to radiate out, and this results in a poor Q factor. The main bottleneck to shrink the cavity volume is the diffraction limit $(\lambda/2n_{\text{eff}})^3$, where λ is the resonant wavelength of the cavity mode, and n_{eff} is an effective refractive index of the cavity. In the past years, many approaches have been proposed to confine light in an ultrasmall region. Those approaches include the defect photonic crystal [2] and microdisk cavities [3]. Another approach is to surround the cavity with metals [4]–[11], and nanolasers with optical pumping or electrical injection were demonstrated. Recently, a room-temperature metal-cavity surface-emitting microlaser has also been demonstrated with continuous-wave operation [12]. So far, the lasing wavelengths of those works mainly range from 0.85 to 1.55 μm. For visible range, a spaser at 525 nm [13] has been demonstrated recently. However, fewer studies have been reported in the visible range.

Metals can reduce the radiative power leakage and effective modal volume. Also, since metals can significantly reduce the optical coupling between adjacent devices, a laser array consisting of metal-coated lasers is expected to exhibit a higher density integration capability than a conventional array of vertical-cavity surface-emitting lasers [14]. This can increase the resolutions of image systems and optical systems of particle manipulation [15]. However, metals also bring the material absorption loss into the cavity. The amount of material loss depends on the polarization of the cavity mode. The surface-wave-like mode with a dominant polarization normal to the metal surface, the so-called plasmonic mode, usually has a higher loss than those of dielectric modes which are mostly well confined in the dielectric part of the cavity. The reason is that a surface wave propagating along the metal/dielectric interface often has a significant portion of the mode profile inside the metal and suffers from more metal loss. The smaller loss makes lasing easier but, with a reduced cavity volume, the loss of the mode tends to increase. Therefore, there is a tradeoff between the cavity volume and Q factor. In this paper, the resonant modes that are more likely to lase are the dielectric modes with a dominant polarization parallel to the metal sidewall. The loss of plasmonic modes is so large that they are hardly resolved spectrally.

Zinc oxide (ZnO) is a material capable of a large gain, and lasing action has been observed in the corresponding nanowires [16]. This material has the potential in other applications such as laser arrays, photodetectors, and switches [17], [18]. Recently, optically pumped ZnO nanodisk lasers with diameters close to their resonant wavelengths have also been experimentally demonstrated [19]. The lasing wavelengths for different sizes of ZnO nanodisks agree well with our theoretical calculations. In this paper, we further investigate the enhancements of Q factor and Γ_E due to metal coating. The emission wavelength corresponding to the bandgap of ZnO is in the ultraviolet regime. Therefore, we consider the metal coating using silver (Ag) and aluminum (Al) because, in the wavelengths of interest, Ag has the smallest imaginary part of the permittivity (the smallest loss) and Al has the largest magnitude of the real part of the permittivity (better field confinement). The comparison for these two metals are carried out with the finite difference time domain (FDTD) method [20], using subpixel smoothing for increased accuracy [21]. The ZnO cavity in our calculation is a hexagonal disk. The resonance wavelengths, Q factors, and mode patterns are

Manuscript received May 5, 2010; revised July 20, 2010 and August 18, 2010; accepted August 28, 2010. Date of current version January 19, 2011. This work was supported in part by the Defense Advanced Research Projects Agency Nanoscale Architecture for Coherent Hyper-Optic Sources Program at the University of Illinois at Urbana-Champaign, Urbana and University of California at Berkeley, Berkeley.

C.-Y. A. Ni, S.-W. Chang, and S. L. Chuang are with the Department of Electrical and Computer Engineering, University of Illinois at Urbana-Champaign, Urbana, IL 61801 USA (e-mail: chiyuni2@illinois.edu; swchang1978@gmail.com; s-chuang@illinois.edu).

D. J. Gargas, M. C. Moore, and P. Yang are with the Department of Chemistry, University of California at Berkeley, Berkeley, CA 94720 USA (e-mail: dgargas@berkeley.edu; michael.moore@berkeley.edu; p_yang@uclink.berkeley.edu).

Color versions of one or more of the figures in this paper are available online at http://ieeexplore.ieee.org.

Digital Object Identifier 10.1109/JQE.2010.2073680

calculated. Based on these parameters, we further estimate the threshold material gain. The results show that the Ag-coated cavity has the smaller threshold material gain. We will also reduce the diameter of the Ag-coated ZnO cavity to study how the Q factor and Γ_E vary with the cavity size.

II. Metal-Coated Hexagonal Cavity

Since ZnO has a wurtzite crystal structure, it forms a hexagonal pillar or disk when grown along the c-axis. Unlike circular cavities covered by a perfect electric conductor (PEC) [22], there are no simple analytical solutions of resonant modes for these hexagonal cavity structures. Although the dependence of the resonance wavelength λ_r and Q factor on the geometry of a 2-D hexagonal cavity have been investigated [23], [24], the plane-wave approximation is not applicable to the 3-D nanodisk cavity, whose size in each dimension is close to the resonance wavelength. In addition, in the 2-D model the radiation loss from the top and bottom of the cavity is neglected, but it becomes important in a 3-D nanodisk.

The main figures of merit for a cavity are the Q factor and energy confinement factor Γ_E, which is roughly the fraction of electromagnetic energy in the active volume [1]

$$\Gamma_\mathrm{E} \equiv \frac{\int_{V_\mathrm{a}} d\mathbf{r}\frac{\epsilon_0}{4}\left[\epsilon_{\mathrm{g,a}}(\mathbf{r},\omega_m)+\epsilon_{\mathrm{R,a}}(\mathbf{r},\omega_m)\right]|\mathbf{E}_m(\mathbf{r})|^2}{\int_{V} d\mathbf{r}\frac{\epsilon_0}{4}\left[\epsilon_{\mathrm{g}}(\mathbf{r},\omega_m)+\epsilon_{\mathrm{R}}(\mathbf{r},\omega_m)\right]|\mathbf{E}_m(\mathbf{r})|^2} \equiv \frac{V_\mathrm{a}}{V_\mathrm{eff}} \tag{1}$$

where the subscript "a" indicates the active gain material, which is the ZnO cavity in our case, m is the mode number of the resonant mode, ϵ_R is the real part of the permittivity, and ϵ_g is the group permittivity defined as

$$\epsilon_\mathrm{g}(\mathbf{r},\omega_m) = \left.\frac{\partial[\omega\epsilon_\mathrm{R}(\mathbf{r},\omega)]}{\partial\omega}\right|_{\omega=\omega_m} \tag{2}$$

which accounts for the dispersion of the materials, especially metal plasma. These two parameters determine the threshold material gain [1]

$$g_\mathrm{th} = \frac{2\pi n_\mathrm{g}}{\Gamma_\mathrm{E} Q\lambda_r} \tag{3}$$

where n_g is the group index of the active material.

From (3), with a high Q factor and a large Γ_E, the threshold material gain is reduced, and so is the threshold carrier density. The Q factor of the cavity mode is related to the radiation leakage and material loss. A high Q factor corresponds to low loss (low threshold gain), while a small value implies that the optical energy decays rapidly because it is easily absorbed by the materials of the cavity or leaks out of the cavity. In our FDTD simulation, the material loss of ZnO is assumed negligible. The loss mechanisms include the radiation leakage and, if coated, metal loss. Coating metal over the cavity can prevent the optical energy from leaking out of the cavity. However, at the same time, the loss from the metal comes into play and influences the total Q factor as well. In our model, these two loss mechanisms are automatically taken into account. The results show that the advantage of reducing the radiation loss by coating metal outweighs the disadvantage of metal loss. In addition, the larger Γ_E due to metal coating leads to the more efficient interaction between photons and carriers, and hence a lower threshold material gain.

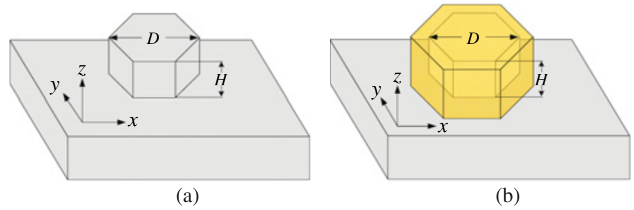

Fig. 1. ZnO nanocavity (a) without and (b) with metal coating. The diameter D (corner-to-corner) and height H of the disk are 727 and 490 nm, respectively, for a submicrometer disk. For the demonstration of metal effect in nanocavities, they are set to 380 and 400 nm, respectively. The metal thicknesses on the sidewall and top are 210 and 100 nm, respectively. The substrate is silicon dioxide.

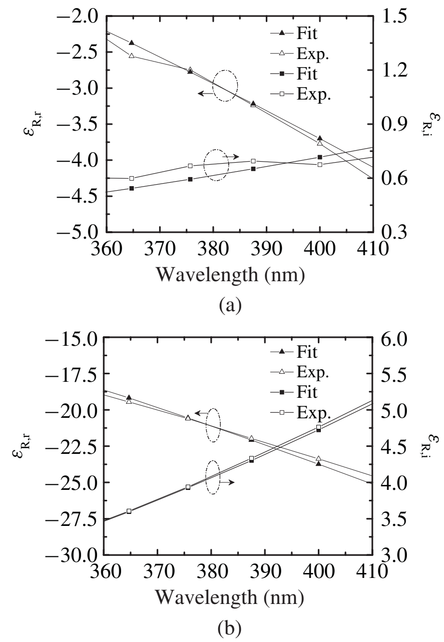

Fig. 2. Relative permittivities of (a) Ag and (b) Al used in this paper and compared with the experimental data [25]. The left and right axes are the real part and imaginary part of the relative permittivity, respectively.

We use FDTD method to find the resonant modes in a 3-D cavity. The cavity structure is shown in Fig. 1. The c-axis of ZnO is defined as the z-axis. We first consider a submicrometer ZnO cavity with a corner-to-corner diameter D and height H of about 727 and 490 nm, respectively. Lasing in such a submicrometer ZnO cavity has been experimentally demonstrated, and the comparison between the experiment and theory for the lasing wavelength can be found in [19]. The refractive index of ZnO is set to 2.4, with the material dispersion neglected. The substrate is silicon dioxide (refractive index $n = 1.5$). The relative permittivities of Ag and Al used in this paper are shown in Fig. 2 and they agree well with the experimental data [25] within a reasonable range.

To search for resonant modes, we place a broadband dipole source in the cavity. By sending a pulse from this dipole source into the cavity, different cavity modes are excited simultaneously. The Q factor and the resonance wavelength of each mode are then calculated from the variation of the electric field with time at one location inside the cavity [26]. To extract the mode pattern of the resonant mode, a narrow-band pulse with the resonance wavelength as the center wavelength is

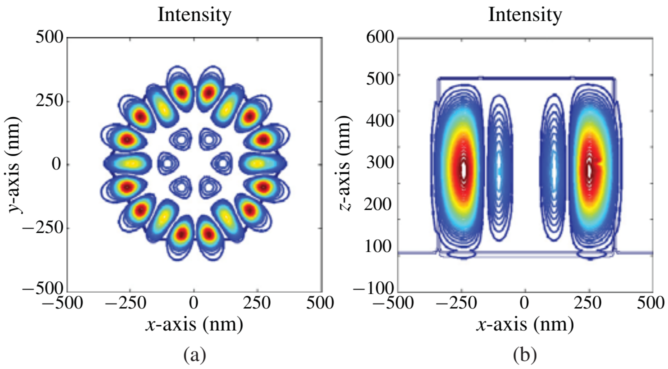

Fig. 3. Calculated mode of a submicrometer disk. The intensity $|\mathbf{E}|^2$ in the (a) xy plane and (b) xz plane, respectively. The mode number is 9. Due to a large diameter, the field can be well confined inside the cavity.

triggered in the cavity again, and the mode pattern is obtained after the source is turned off. Based on these procedures, we find the cavity mode with a resonance wavelength of 386.1 nm. Due to this large diameter, the azimuthal mode number m is 9, the Q factor is 297.4, the energy confinement factor Γ_E is 0.91, and the corresponding material threshold gain estimated from (3) is 1427.1 cm^{-1}, which is achievable for ZnO under a reasonable pumping power. The corresponding mode pattern is shown in Fig. 3. This mode is transverse magnetic (TM)-like with the dominant polarization parallel to the z-axis. Due to its TM-like characteristics, this mode has a high reflectivity and a high Q factor.

To demonstrate the advantage of metal, we consider a cavity with an even smaller diameter and height than those of the ZnO cavity in the previous case. For the bare disk in Fig. 1(a) but with a corner-to-corner diameter and height of 380 and 400 nm, respectively, we obtain a resonant mode with the azimuthal mode number $m = 4$. The corresponding resonance wavelength lies within the gain spectrum of ZnO. In addition, in our mode search, we find only the TM-like mode. This can be understood as a result of the larger reflectivity of the TM-like mode than that of the transverse electric (TE)-like (polarization parallel to the growth plane) mode, and hence the TE-like mode decays faster due to the larger power leakage, especially for such a small cavity. Thus, the TM-like mode has a larger Q factor. The TM-like mode has a resonance wavelength of 404.9 nm and Q factor of about 40.81. Compared to the large cavity in the previous case, we see that the cavity size significantly influences the Q factor and the field confinement. Since in our model there is no material loss in ZnO, the reduction of the Q factor is entirely caused by the increase of the radiation loss, which means that with the reduction of the cavity volume, power leaks out more easily [19]. In addition, the resonant mode tends to spill out in the smaller cavity, which reduces Γ_E, as manifested by the comparison between the mode patterns of this cavity [Fig. 4(a) and (b)] and those of the larger one (Fig. 3). This comparison indicates the challenge of further shrinking the cavity without any metal coating, though it is not impossible [19].

We then calculate the Q factors, energy confinement factors, and resonance wavelengths of the cavity modes with the same azimuthal mode number m in different metal-coated cavities.

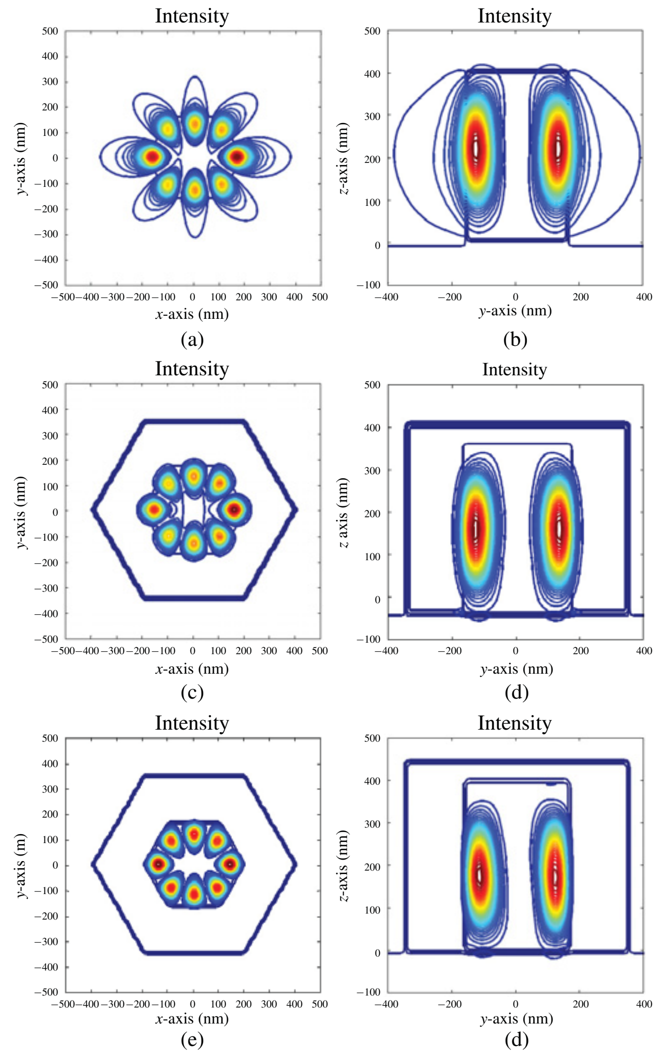

Fig. 4. Mode intensity $|\mathbf{E}|^2$ distributions inside the cavity without metal coating on (a) xy plane and (b) yz plane. The counterparts of the Ag-coated cavity are shown in (c) and (d), and those of the Al-coated cavity are shown in (e) and (f). In all these cavities, the modes are TM-like.

The permittivity of metal is adopted from [25]. We focus on the comparison between two coating metals Ag and Al. The real part of the Al permittivity is more negative than that of Ag, and the imaginary part of Al permittivity is also larger than that of Ag. The former means that more field will be reflected back to the cavity, but the latter implies that the more energy is dissipated in each optical period, and thus a larger material loss. The Q factor will be determined by these two mechanisms. In the metal-coated cavity, the TE-like mode cannot be found. The absences of TE-like modes in Al and Ag have different origins. In the Al-coated cavity, the TE-like mode is a plasmonic mode. With the reduction of cavity volume, the modal loss of the plasmonic mode increases significantly, and this mode has a small Q factor and cannot be resolved spectrally. The dependence of the Q factor on the polarization in the metal-coated microcavity has been experimentally demonstrated [27], and our calculation indicates the same outcome. As for Ag-coated cavity, since the magnitude of the real part of Ag permittivity in this wavelength regime is smaller than that of ZnO, the surface wave cannot exist.

TABLE I
COMPARISON AMONG THREE ZnO NANOCAVITIES: BARE DISK, Al-COATED, AND Ag-COATED ZnO DISKS

Structure	λ (nm)	Γ_E	Q	g_{th} (cm^{-1})
Bare disk	404.9	0.55	40.8	16 613.2
Al-coated	363.3	0.97	89.0	4831.0
Ag-coated	385.0	0.95	128.0	3206.5

Therefore, the TE-like mode in Ag-coated cavity is not a plasmonic mode, and it suffers from both radiation loss and absorption loss. Moreover, the power reflectivity of the TE-like mode is smaller than that of the TM-like mode. Due to these two loss mechanisms, we deduce that the presence of the TE-like mode is very short-lived in the Ag-coated cavity.

For the Al-coated cavity, the TM-like mode has a Q factor and resonance wavelength of 89 and 363.34 nm, respectively, and the counterparts of the Ag-coated cavity are 128 and 385 nm. Their mode patterns are shown in Fig. 4(c)–(f).

The relative permittivities are $-18.9 + 3.54i$ and $-3.1 + 0.64i$ for Al and Ag at the respective resonance wavelengths (see Fig. 2). From Fig. 4, in the case of the cavity without metal coating, most of the field radiates out into air. However, as the cavity is coated with the metal, field can be well confined in the ZnO nanodisk. Furthermore, the field is confined better in the Al-coated cavity. We obtain $\Gamma_E = 0.97$ from (1) for the Al-coated cavity, which is slightly larger than a value of 0.95 for the Ag-coated cavity. The better mode confinement of Al-coated cavity is due to the larger magnitude of the real part of the Al permittivity in this wavelength range, which pushes the field back into ZnO nanodisk and is consistent with the higher power reflectivity at the sidewall of the Al-coated cavity. However, the higher Γ_E does not always mean a higher Q factor since the mode also suffers from the absorption loss from metal. In this case, the imaginary part of Al permittivity is much larger than that of Ag, and this actually leads to a smaller Q factor for the Al-coated cavity. We then calculate the threshold material gain according to (3). The comparison among these three cases is shown in Table I. From Table I, the resonance wavelength shifts to the shorter wavelength side when Γ_E becomes larger. To understand this, we consider the following dispersion relation:

$$k^2 = \left(\frac{2\pi n}{\lambda}\right)^2 = k_t^2 + k_z^2 \tag{4}$$

where k is the wave number in ZnO, and k_t as well as k_z are the wave numbers in the transverse and z directions, respectively. The field in the Al-coated cavity is better confined. Therefore, its fields in the transverse and z directions vary the fastest among the three cases, namely, k_t and k_z of the Al-coated cavity are the largest among those of the three cavity modes. Conversely, in the bare nanodisk, the field tends to extend into air and varies slowly. Therefore, its k_t and k_z are the smallest. The larger k corresponds to the higher resonance frequency (shorter resonance wavelength). Therefore, the cavity mode of the Al-coated cavity has the shortest resonance wavelength.

From Table I, the threshold material gains of the metal-coated cavities are smaller than those of the uncoated cavity by about four times. The reason is that the metal significantly suppresses the radiation loss, while the accompanying material loss is much smaller than this loss reduction. Thus, the Q factor is doubled (Al) or tripled (Ag). Meanwhile, Γ_E is also significantly improved by a factor of two. These two improvements lead to a smaller threshold material gain. The threshold material gain of the Al-coated cavity is higher than that of the Ag counterpart because Al has the larger material loss. To further reduce the material loss from the metal, the temperature of the coated cavity could be lowered, and the threshold material gain can decrease accordingly.

Although the total volume of the metal-coated cavity is comparable to that of the submicrometer cavity ($D = 726$ nm, $H = 490$ nm), it is fairer to compare the effective modal volume V_{eff}, which can be calculated from (1). The effective modal volumes of the submicrometer, small bare-disk, Al-coated, and Ag-coated cavities are 1.85×10^8, 6.82×10^7, 3.86×10^7, and 3.95×10^7 nm^3, respectively. Comparing the cases of submicrometer cavity and Ag-coated cavity, we find that the effective modal volume V_{eff} is reduced to one-fourth at the expense of twice the threshold material gain. On the other hand, the comparison of small bare-disk and Ag-coated cavities indicates that V_{eff} is reduced to around one-half, and the threshold material gain is significantly decreased to a quarter or even less. These results show the advantage of metals in shrinking the effective modal volume.

Nevertheless, it should be pointed out that metal coating does not always improve Q factor and Γ_E, especially when the cavity size is large enough. For big devices, the optical field is already well confined in the cavity, and metal coating simply increases the material loss. In this case, instead of suppressing radiation loss, coating metal degrades the performance of the cavity.

III. SHRINKING CAVITY VOLUME WITH Ag

In Table I, the Ag-coated cavity exhibits the smallest threshold material gain, and smallest ratio of the effective mode volume V_{eff} to $(\lambda/2n_{\mathrm{eff}})^3$ is 75.4 ($n_{\mathrm{eff}} = 2.4$). In this section, we investigate the dependence of Q factor and Γ_E on the diameter of the Ag-coated cavity. The height H could change the Q factor and Γ_E. However, the variation of Q factor is around 15%, and the change of Γ_E is small for a given mode. Therefore, it does not drastically influence the trends, and we set the height to 400 nm in each case. The fixing of height also makes the comparison simpler because only one parameter is varied. The resonant wavelength of the mode with a high Q factor tends to blue-shift and may not fall in the gain spectrum. Hence, we only consider the modes with wavelengths within the range of interest although they might not be of same type. The results are shown in Fig. 5, and the details are tabulated in Table II. At $D = 160$ nm, we see the ratio $V_{\mathrm{eff}}/(\lambda/2n_{\mathrm{eff}})^3$ can be as small as 23.9.

The resonant modes in $D = 160$, 260, and 380 nm are TM_{110}, TM_{020}, and TM_{410} modes, where we label the modes according to their similarities with those of a cylindrical circular cavity covered by PEC. To understand how the resonant mode evolves, we plot the resonance wavelength vs. radius for

TABLE II
COMPARISON AMONG THREE Ag-COATED ZnO DISKS WITH DIFFERENT DIAMETERS

D (nm)	λ (nm)	Γ_E	$V_{eff}/(\lambda/2n_{eff})^3$	Q	g_{th} (cm^{-1})
160	378	0.69	23.9	42	13 809
260	384	0.78	53.2	58	8617
380	385	0.95	75.4	128	3207

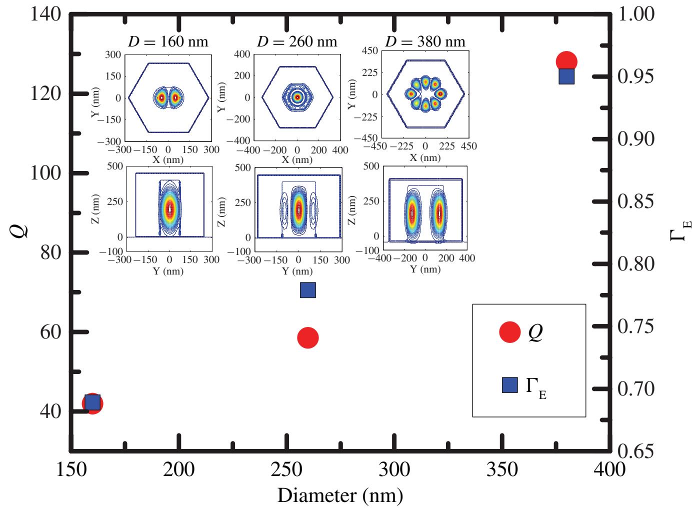

Fig. 5. Q factor (left axis) and the energy confinement factor Γ_E (right axis). The intensity distribution of each mode is shown in the insets. The figures in the top and bottom rows are the intensity distributions in the xy and yz planes, respectively.

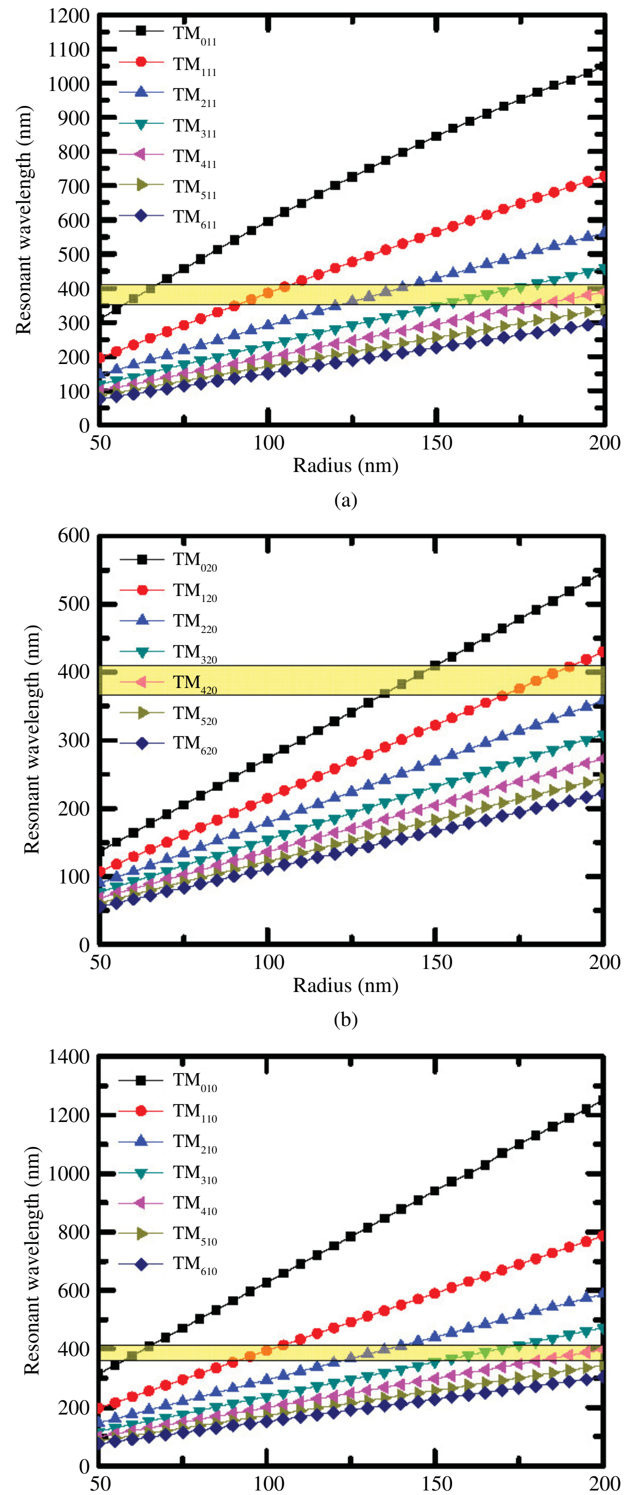

Fig. 6. Dispersion curves of (a) TM_{m11}, (b) TM_{m20}, and (c) TM_{m10} modes. The yellow region indicates the spectral range of interest.

the TM_{m11}, TM_{m20}, and TM_{m10} modes [22]

$$\lambda_{r,mnp} = \frac{2\pi\sqrt{\epsilon}}{\sqrt{\left(\frac{\chi_{mn}}{R}\right)^2 + \left(\frac{p\pi}{H}\right)^2}} \tag{5}$$

where ϵ is the relative permittivity of ZnO, R is the radius defined as the distance from the center to the corner, H is the height of the cavity, and χ_{mn} is the zero of the Bessel function $J_m(x)$.

Although (5) is only valid for the TM modes in a circular PEC cavity, it can predict the resonant wavelength of the corresponding modes in the wavelength of interest for the metal-coated ZnO cavity. The deviation of the numerical values in (5) can result from the hexagonal shape and differences of Ag and substrate from PEC in this wavelength range. The skin depth in the metal and the penetration depth into the substrate are more significant with the decrease of the diameter. Therefore, the effective radius and height are slightly larger than the physical values, which give rise to longer resonant wavelengths from FDTD calculation when compared to those obtained from (5). Nevertheless, (5) provides a good guidance for mode search, while other parameters such as Q factor still require FDTD calculations.

For examples, Fig. 6 shows that possible modes are TM_{410} and TM_{411} at a radius $R = 190$ nm ($D = 380$ nm). We do not show the mode profile of TM_{411} mode in Fig. 5 since it has the smaller Q factor around 81 as a result of more power leakage into the substrate (relatively large magnitude of k_z). The same reason applies to the case of $R = 80$ nm ($D = 160$ nm). In that case, the possible resonant modes are TM_{110} and TM_{111}, and similarly the TM_{110} mode has the larger Q factor. When the radius is 130 nm ($D = 260$ nm), TM_{211}, TM_{020}, and TM_{210} modes can all exist in the spectral range of interest.

However, the TM_{020} mode is the one with the highest Q factor because this mode tends to bounce back and forth in the radial direction (more nodes in the radial direction and thus larger k_t) rather than leaking out into the substrate.

From Fig. 5, we see that the Q factor and Γ_E decrease with the diameter. Since the cavity is coated with the same metal, a small Γ_E means that more field either resides in the metal (the material loss) or penetrates into the substrate (the radiation loss), and therefore, the Q factor decreases. From the inset in Fig. 5, the field is gradually pushed into metal as the diameter decreases. At $D = 160$ nm, the field is not only pushed into metal but also leaks into the substrate. Thus, there are more material and radiation losses. However, the required threshold material gains in these three cases are still smaller than that of the bare disk with a diameter of 380 nm. This implies that metal can be beneficial to the reduction of optical modal volume.

Further reduction of the effective mode volume of TM-like mode with metal coating is restricted by the real part of the metal permittivity in this wavelength range. If the magnitude of the real part of the metal permittivity can be larger, the cavity volume can be further reduced. This makes the application of metal at the near-infrared regime more promising because the magnitude of the real part of Ag permittivity can be more than 100 at that wavelength range. Despite the larger imaginary part of the metal permittivity at the near-infrared range, the even more negative real part may limit the amount of field inside metal and maintain a reasonable Q factor. However, to further break the diffraction limit, the plasmonic mode may have more potential.

IV. Conclusion

In this paper, we have theoretically studied the effect of coating metal on ZnO nanocavities. We showed that the metal coating can have a positive impact on the Q factor, optical energy confinement factor Γ_E, and threshold material gain of the modes in a ZnO nanocavity.

The threshold material gain increases rapidly as the bare cavity volume decreases. We showed that metal coating can improve the Q factor and energy confinement factor Γ_E of the modes in a ZnO nanocavity. The increase of the Q factor and better field confinement from Ag reduce the threshold material gain by a factor of four when compared to those of the uncoated cavity. The effective modal volume V_{eff} is also reduced to around half of that for the uncoated cavity. The resonance wavelength shift was also investigated on the basis of the dispersion relation. We then studied the possibility of shrinking cavity volume with Ag around the wavelength 370–410 nm. The ratio of V_{eff} over $(\lambda/2n_{\mathrm{eff}})^3$ can be as small as 23.9 at a diameter of 160 nm.

References

[1] S.-W. Chang and S. L. Chuang, "Fundamental formulation for plasmonic nanolasers," *IEEE J. Quantum. Electron.*, vol. 45, no. 8, pp. 1014–1023, Aug. 2009.

[2] K. Nozaki, H. Watanabe, and T. Baba, "Photonic crystal nanolaser monolithically integrated with passive waveguide for effective light extraction," *Appl. Phy. Lett.*, vol. 92, no. 2, pp. 021108-1–021108-3, Jan. 2008.

[3] N. C. Frateschi and A. F. J. Levi, "The spectrum of microdisk lasers," *J. Appl. Phys.*, vol. 80, no. 2, pp. 644–653, Jul. 1996.

[4] S. A. Maier, "Effective mode volume of nanoscale plasmon cavities," *Opt. Quantum Electron.*, vol. 38, nos. 1–3, pp. 257–267, Jan. 2006.

[5] E. Feigenbaum and M. Orenstein, "Optical 3-D cavity modes below the diffraction-limit using slow-wave surface-plasmon-polaritons," *Opt. Exp.*, vol. 15, no. 5, pp. 2607–2612, Mar. 2007.

[6] C. Manolatou and F. Rana, "Subwavelength nanopatch cavities for semiconductor plasmon lasers," *IEEE J. Quantum Electron.*, vol. 44, no. 5, pp. 435–447, May 2008.

[7] M. T. Hill, Y.-S. Oei, B. Smalbrugge, Y. Zhu, T. de Vries, P. J. van Veldhoven, F. W. M. van Otten, T. J. Eijkemans, J. P. Turkiewicz, H. de Waardt, E. J. Geluk, S.-H. Kwon, Y.-H. Lee, R. Nötzel, and M. K. Smit, "Lasing in metallic-coated nanocavities," *Nature Photon.*, vol. 1, no. 10, pp. 589–594, Sep. 2007.

[8] M. T. Hill, M. Marell, E. S. Leong, B. Smalbrugge, Y. Zhu, M. Sun, P. J. Veldhoven, E. J. Geluk, F. Karouta, Y. S. Oei, R. Nötzel, C. Z. Ning, and M. K. Smit, "Lasing in metal-insulator-metal sub-wavelength plasmonic waveguides," *Opt. Exp.*, vol. 17, no. 13, pp. 11107–11112, Jun. 2009.

[9] A. Mizrahi, V. Lomakin, B. A. Slutsky, M. P. Nezhad, L. Feng, and Y. Fainman, "Low threshold gain metal coated laser nanoresonators," *Opt. Lett.*, vol. 33, no. 11, pp. 1261–1263, Jun. 2008.

[10] M. P. Nezhad, A. Simic, O. Bondarenko, B. Slutsky, A. Mizrahi, L. Feng, V. Lomakin, and Y. Fainman, "Room-temperature subwavelength metallo-dielectric lasers," *Nature Photon.*, vol. 4, no. 6, pp. 395–399, Apr. 2010.

[11] K. Yu, A. Lakhani, and M. C. Wu, "Subwavelength metal-optic semiconductor nanopatch lasers," *Opt. Exp.*, vol. 18, no. 9, pp. 8790–8799, Apr. 2010.

[12] C.-Y. Lu, S.-W. Chang, S. L. Chuang, T. D. Germann, and D. Bimberg, "Metal-cavity surface-emitting microlaser at room temperature," *Appl. Phys. Lett.*, vol. 96, no. 25, pp. 251101-1–251101-3, Jun. 2010.

[13] M. A. Noginov, G. Zhu, A. M. Belgrave, R. Bakker, V. M. Shalaev, E. E. Narimanov, S. Stout, E. Herz, T. Suteewong, and U. Wiesner, "Demonstration of a spaser-based nanolaser," *Nature*, vol. 460, no. 7259, pp. 1110–1112, Aug. 2009.

[14] C. L. Chua, R. L. Thornton, D. W. Treat, and R. M. Donaldson, "Independently addressable VCSEL arrays on 3-μm pitch," *IEEE Photon. Technol. Lett.*, vol. 10, no. 7, pp. 917–919, Jul. 1998.

[15] A. Kroner, F. Rinaldi, R. Rösch, and R. Michalzik, "Optical particle manipulation by application-specific densely packed VCSEL arrays," *Electron. Lett.*, vol. 44, no. 5, pp. 353–354, Feb. 2008.

[16] M. H. Huang, S. Mao, H. Feick, H. Yan, Y. Wu, H. Kind, E. Weber, R. Russo, and P. Yang, "Room-temperature ultraviolet nanowire nanolasers," *Science*, vol. 292, no. 5523, pp. 1897–1899, Jun. 2001.

[17] L. E. Greene, M. Law, D. H. Tan, M. Montano, J. Goldberger, G. Somorjai, and P. Yang, "General route to vertical ZnO nanowire arrays using textured ZnO seeds," *Nano Lett.*, vol. 5, no. 7, pp. 1231–1236, Jun. 2005.

[18] H. Kind, H. Yan, B. Messer, M. Law, and P. Yang, "Nanowire ultraviolet photodetectors and optical switches," *Adv. Mater.*, vol. 14, no. 2, pp. 158–160, Jan. 2002.

[19] D. J. Gargas, M. C. Moore, A. Ni, S.-W. Chang, Z. Zhang, S.-L. Chuang, and P. Yang, "Whispering gallery mode lasing from zinc oxide hexagonal nanodisks," *ACS Nano*, vol. 4, no. 6, pp. 3270–3276, Apr. 2010.

[20] A. Taflove and S. C. Hagness, *Computational Electrodynamics: The Finite-Difference Time-Domain Method*. Norwood, MA: Artech House, 2000.

[21] A. Farjadpour, D. Roundy, A. Rodriguez, M. Ibanescu, P. Bermel, J. D. Joannopoulos, S. G. Johnson, and G. W. Burr, "Improving accuracy by subpixel smoothing in FDTD," *Opt. Lett.*, vol. 31, no. 20, pp. 2972–2974, Oct. 2006.

[22] C. A. Balanis, *Advanced Engineering Electromagnetics*, 1st ed. New York: Wiley, 1989.

[23] J. Wiersig, "Hexagonal dielectric resonators and microcrystal lasers," *Phys. Rev. A*, vol. 67, no. 2, pp. 023807-1–023807-12, Feb. 2003.

[24] A. K. Bhowmik, "Polygonal optical cavities," *Appl. Opt.*, vol. 39, no. 18, pp. 3071–3075, Jun. 2005.

[25] E. D. Palik, *Handbook of Optical Constants of Solids*. New York: Academic, 1985.

[26] V. A. Mandelshtam and H. S. Taylor, "Harmonic inversion of time signals and its applications," *J. Chem. Phys.*, vol. 107, no. 17, pp. 6756–6769, Nov. 1997.

[27] B. Min, E. Ostby, V. Sorger, E. Ulin-Avila, L. Yang, X. Zhang, and K. Vahala, "High-Q surface-plasmon-polariton whispering-gallery microcavity," *Nature*, vol. 457, no. 7228, pp. 455–458, Jan. 2009.

Chi-Yu Adrian Ni received the B.S. degree in electrical engineering and the M.S. degree in photonics and optoelectronics from the National Taiwan University, Taipei, Taiwan, in 2000 and 2002, respectively. He is currently pursuing the Ph.D. degree in the Department of Electrical and Computer Engineering, University of Illinois at Urbana-Champaign, Urbana.

His current research interests include semiconductor physics, mainly in optoelectronics, including plasmonic devices, lasers, and modulators.

Shu-Wei Chang (M'09) received the B.S. degree in electrical engineering from the National Taiwan University, Taipei, Taiwan, in 1999, and the M.S. and Ph.D. degrees from the Department of Electrical and Computer Engineering, University of Illinois at Urbana-Champaign, Urbana, in 2003 and 2006, respectively.

He is currently with the Department of Electrical and Computer Engineering, University of Illinois at Urbana-Champaign. His current research interests include fundamental and applied physics of semiconductor photonics including tunneling-injection quantum-dot–quantum-well coupled systems, slow and fast light in semiconductor nanostructures, spin relaxation in strained [110] and [111] semiconductor quantum wells, group-IV direct-bandgap semiconductor lasers, active and passive plasmonic devices, and semiconductor nanolasers.

Dr. Chang is a member of the Optical Society of America. He was the recipient of the John Bardeen Memorial Graduate Award from the Department of Electrical and Computer Engineering, University of Illinois at Urbana-Champaign, in 2006.

Daniel J. Gargas received the B.S. degree in chemistry and mathematics from the University of Puget Sound, Tacoma, WA, in 2000, and the Ph.D. degree in chemistry from the University of California, Santa Barbara, in 2007.

He has been working as a Post-Doctoral Researcher in Prof. P. Yang's Group at the University of California, Berkeley, since 2007. His current research interests include the integration and study of plasmonic-enhanced optical processes in nanostructured photonic materials.

Michael C. Moore received the B.A. degree in chemistry from Oberlin College, Oberlin, OH, in 2006. He is currently pursuing the Ph.D. degree in chemistry at the University of California, Berkeley.

His current research interests include the growth and optical properties of nanostructured semiconductors.

Peidong Yang received the B.S. degree in chemistry from the University of Science and Technology, Anhui, China, in 1993, and the Ph.D. degree in chemistry from Harvard University, Cambridge, MA, in 1997.

He was a Post-Doctoral Research Fellow at the University of California, Santa Barbara, before joining the faculty in the Department of Chemistry, University of California, Berkeley, in 1999. He is currently a Professor in the Department of Chemistry, Materials Science and Engineering and a Senior Faculty Scientist at the Lawrence Berkeley National Laboratory, Berkeley, CA. He is also the Deputy Director of the Center of Integrated Nanomechanical Systems, Berkeley. His current research interest include 1-D semiconductor nanostructures and their applications in nanophotonics, nanoelectronics, energy conversion, and nanofluidics.

Dr. Yang is a recipient of the Alfred P. Sloan Research Fellowship, the Arnold and Mabel Beckman Young Investigator Award, the National Science Foundation Young Investigator Award, the Materials Research Society (MRS) Young Investigator Award, the Julius Springer Prize for Applied Physics, the American Chemical Society (ACS) Pure Chemistry Award, and the Alan T. Waterman Award. He was the first Chairperson of the Nanoscience Subdivision of ACS. He was recently elected an MRS Fellow. He is an Associate Editor for *Journal of the ACS* and also serves on the Editorial Advisory Board for number of journals including *Accounts of Chemical Research* and *Nano Letters*.

Shun Lien Chuang (S'78–M'82–SM'88–F'97) received the B.S. degree from the National Taiwan University, Taipei, Taiwan, in 1976, and the M.S., E.E., and Ph.D. degrees from the Massachusetts Institute of Technology, Cambridge, in 1980, 1981, and 1983, respectively, all in electrical engineering.

He is currently the Robert MacClinchie Distinguished Professor in the Department of Electrical and Computer Engineering, University of Illinois at Urbana-Champaign, Urbana. He was a visitor at the AT&T Bell Laboratories, Holmdel, NJ, in 1989, the Sony Research Center, Yokohama, Japan, in 1995, and the NTT Basic Research Laboratories, Atsugi, Japan, in 1997. He was also a visitor at the NASA Ames Research Center, Moffett Field, CA, in 1999, the Fujitsu Research Laboratories, Atsugi, Japan, in 2000, the Cavendish Laboratory, University of Cambridge, Cambridge, England, in 2002, and the Technical University of Berlin, Berlin, Germany, in 2009. He is the author of *Physics of Photonic Devices* (2nd ed., Wiley, 2009) and *The Physics of Optoelectronic Devices* (Wiley, 1995). He has published more than 300 journal articles and conference papers, and has delivered many invited talks at conferences and institutions. His current research interests include nanolasers, plasmonics, strained semiconductor quantum-well and quantum-dot lasers, and superlattice photodetectors.

Dr. Chuang is a Fellow of the American Physical Society and the Optical Society of America (OSA). He has been cited frequently in the list of excellence in teaching at the University of Illinois. He was awarded a Fellowship from the Japan Society for the Promotion of Science to visit the University of Tokyo in 1996. He received the Engineering Excellence Award from the OSA in 2004, the IEEE Lasers and Electro-Optical Society (LEOS) Distinguished Lecturer Award for the period 2004–2006 for two terms, and the William Streifer Scientific Achievement Award from IEEE LEOS in 2007. He received the Humboldt Research Award for Senior U.S. Scientists for the period 2008–2009. He was elected as a member of the Board of Governors for IEEE Photonics Society for 2009–2011. He served as an Associate Editor of the IEEE JOURNAL OF QUANTUM ELECTRONICS from 1997–2002, and the *Journal of Lightwave Technology* from 2007–2008. He was a General Co-Chair for the Slow and Fast Light Meeting of the OSA in July 2008, and has served in many technical program committees of IEEE and the OSA. He was a Feature Editor for a special issue of the *Journal of the Optical Society of America B* on terahertz generation, physics, and applications in 1994. He also edited a feature section on mid-infrared quantum cascade lasers in the June 2002 issue of the *Journal of Quantum Electronics*.